Interfacial mixing in heteroepitaxial growth

Boris Bierwald,[1] Michael von den Driesch,[1] Zéno Farkas,[1] Sang Bub Lee,[1,2] and Dietrich E. Wolf[1]
[1]*Institut für Physik, Universität Duisburg-Essen, D-47048 Duisburg, Germany*
[2]*Department of Physics, Kyungpook National University, Taegu, 702-701, Korea*
(Received 3 June 2003; revised manuscript received 3 May 2004; published 19 August 2004)

We investigate the growth of a film of some element B on a substrate made of another substance A in a model of molecular beam epitaxy. A vertical exchange mechanism (partial surfactant behavior) allows the A atoms to stay on the growing surface with a certain probability. Using kinetic Monte Carlo simulations as well as scaling arguments, the incorporation of the A's into the growing B layer is investigated. Moreover, we develop a rate equation theory for this process. The concentration of A impurities decays in the B-film like $(\text{distance from the interface})^{-1-\beta}$, where $\beta \approx 0.5$ for two-dimensional surfaces, ≈ 0.8 in the one-dimensional case, and 1 in mean-field approximation. The power law is cut off exponentially at a characteristic thickness of the interdiffusion zone that depends on the rate of exchange of a B adatom with an A atom in the surface and on the diffusion length. Under certain conditions the interdiffusion zone is predicted to become narrower, if the growth temperature is increased.

DOI: 10.1103/PhysRevE.70.021604 PACS number(s): 81.15.Aa, 68.35.Fx, 81.15.Kk

I. INTRODUCTION

Heterolayers, where, e.g., ferromagnets are in contact with antiferromagnets, semiconductors or superconductors, give rise to ordering and transport phenomena, which depend crucially on the interfacial structure. Examples for such ordering phenomena are the exchange bias [1], or the cryptomagnetism [2]. Electronic transport through a ferromagnetic-nonmagnetic-ferromagnetic sandwich ("spin valve" geometry) gives rise to the giant magnetoresistance [3,4]. Another example is the recently predicted possibility to enhance or reduce a Josephson current magnetically by replacing the tunnel barrier of a Josephson junction by a ferromagnetic-insulating-ferromagnetic sandwich [5]. These phenomena belong to the growing field of spintronics [6], where the spin degree of freedom is used for electronic signal processing. Interfacial mixing affects all of them [7]. For example, it leads to spin scattering disturbing the spin dependent transport properties.

Therefore, it is important to be able to control the various physical processes that may spoil sharp interfaces. Some of them proceed after growth such as bulk interdiffusion or chemical interface reactions like silicide formation. However, diffuse interfaces may also be caused by processes taking place exclusively at the surface: For example, the substrate may partially behave like a surfactant when one grows a different material on it. It is this latter mechanism which we investigate in this paper. The questions we want to answer concern the asymptotic concentration profile, the width of the interdiffusion zone and possible correlations among the substrate impurities within the growing layer.

Specifically we consider growing some material B on a substrate A. Obviously interfacial mixing requires that some substrate (A) atoms get replaced by B atoms and "float up" on the surface until they get incorporated into the growing film. Often the rate for the reverse process is so small that it can be neglected. Such a behavior occurs, e.g., for Cr on Fe [8], AlAs on GaAs [9], Nb on Fe [10], and Au on Fe [11].

This surfactant-like behavior depends on the interaction between the different atoms including magnetic contributions and lattice mismatch. In particular the explanation of any ordering of A and B atoms close to the interface would require a detailed investigation of these interactions [12]. The situation becomes considerably simpler, however, if one is interested in the physical properties further away from the interface. Then the concentration of A atoms may be regarded as sufficiently low that their interaction as well as A-B ordering become unimportant. The focus on this region justifies our simplified model in which the surfactant-like behavior of A atoms is described by a constant rate E with which a B adatom exchanges irreversibly with an A atom in the crystal layer below. This means that B atoms are more strongly bound in a B environment than A atoms, which get expelled onto the free surface if a B atom is available to take their place.

Apart from the exchange there is a second crucial ingredient in the model: The A atoms behave only *partially* as a surfactant in the sense that they can be overgrown by island edges. By contrast a perfect surfactant atom should float up also in front of an advancing island edge.

Further phenomenological parameters characterizing the model are the deposition rate F of B atoms and the diffusion constants D_A and D_B of the adatoms of type A or B, respectively. The limit $E/D_B \to \infty$, where a B adatom exchanges with the first A atom it encounters, would be realized if the B adatoms diffuse by an exchange mechanism [13] while the A adatoms diffuse by hopping.

In the present paper we make two assumptions which are generally not fulfilled and can affect the physical behavior substantially. What will change if these model restrictions are relaxed, will be discussed in Sec. IX. The first simplification is that both kinds of atoms diffuse equally fast on the surface, $D_A = D_B = D$, with a diffusion constant independent of the surface composition. The second simplification is that Ehrlich-Schwoebel barriers are not taken into account: Diffusion on a terrace and across a terrace edge are described by the same diffusion constant D. This turns out to be justified

for weak enough Ehrlich-Schwoebel barriers. We make these assumptions because we want the nucleation of islands on the surface to be goverened by a single diffusion length. Crossover phenomena to be expected if there are other competing length scales would make a quantitative investigation of interfacial mixing much more difficult so that it is legitimate to consider this limiting case first.

Naively one would expect an exponential decay of the density profile of A atoms far from the interface. It is the main result of this investigation that this is not always the case: The incorporation of A atoms is much slower, giving rise to a power law decay of the concentration profile in the limit of perfect layer-by-layer growth, $D/F \to \infty$. In this case the width of the interdiffusion zone diverges, provided there are no finite size effects. By contrast we shall show that for finite D/F the width of the interdiffusion zone is no longer infinite, but a power law of D/F.

This paper is organized as follows. In the next section we are going to define a simple solid-on-solid (SOS) model for epitaxial growth of a B layer on an A substrate, which allows for the irreversible exchange of B atoms with A's at the surface. In this model the A atoms on the surface turn out to cluster in a time-periodic self-organized way, which is explained in Sec. III. The next three sections, Secs. IV–VI, are devoted to the limit of perfect layer-by-layer growth, $D/F \to \infty$. First, in Sec. IV, we present a simple mean field argument leading to the prediction, that the concentration of A's decays algebraically in the B layer. For a finite system size this power law is cut off leading to a finite width H of the interdiffusion zone, which is discussed in Sec. V, where also a scaling ansatz for the surface concentration c_A is proposed. This scaling ansatz is confirmed by simulation results for one- and two-dimensional surfaces in Sec. VI. The remaining sections deal with interdiffusion for finite D/F. Section VII contains simulation results and scaling arguments, and in Sec. VIII a rate equation theory is developed for the interdiffusion problem. Possible refinements of our model are discussed in the conclusion, Sec. IX. In the Appendix we describe a very efficient implementation of the simulation model for one-dimensional surfaces in the limit $D/F \to \infty$.

II. THE MODEL

In order to study interfacial mixing in heteroepitaxial growth of a B layer on an A substrate we introduce a simple SOS model defined on a simple cubic lattice by the following kinetic rules (cf. Fig. 1).

(1) Starting from an initially flat substrate consisting of A atoms, B atoms are deposited at randomly selected sites on the surface with deposition rate F.

(2) As long as they do not have a lateral neighbor, the B atoms diffuse on the surface with diffusion constant D.

(3) When such a B atom happens to sit on top of an A atom, it can exchange vertically with rate E or continue to diffuse with rate D.

(4) After an exchange, the B atom stays irreversibly bound, whereas the A atom diffuses on the surface with diffusion constant D.

(5) There is *no* back exchange, when an A atom sits on top of a B atom.

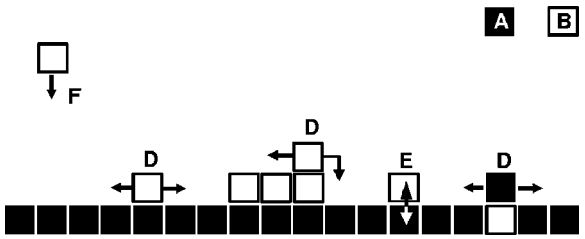

FIG. 1. The growth model. B atoms are deposited with a deposition rate F onto the substrate. Adatoms diffuse on the surface and down to the binding site at an island edge with diffusion constant D irrespective of their type. In the top layer mobile B's can exchange with A's with an effective exchange rate E.

(6) When two adatoms, regardless of their type, meet, they form a stable immobile nucleation center of an island.

(7) When an adatom, regardless of its type, reaches a site adjacent to an island, it is irreversibly bound, increasing the size of the island.

(8) Both types of particles can diffuse down across terrace edges without being hindered by an Ehrlich-Schwoebel barrier.

(9) There are no overhangs, i.e., we assume SOS growth.

(10) The exchange of a B atom, with an A atom underneath is forbidden, if the B-atom is already part of an island, i.e., if it has a nearest neighbor at the same height. Hence, A atoms can be overgrown by island edges.

Rules (4)–(7) violate detailed balance. Irreversible binding and the absence of reincorporation of an expelled A atom into the B surface underneath are justified, if the dissociation and reincorporation rates are so small that these processes hardly ever happen within the layer completion time, $t_F = 1/Fa^2$. This is the time, during which the film grows by one monolayer. The dynamics of buried atoms is usually much slower than that of surface atoms and is not considered here. In this sense, the system never approaches thermal equilibrium, as long as the deposition rate Fa^2 is large enough compared to the rates we neglect.

Measuring time in units of the monolayer completion time t_F one can identify the average film thickness (the B dose in monolayers) with the deposition time. Choosing in addition the lattice constant a as length unit, this model is controlled by the two dimensionless parameters D/Fa^4 and $r_E \equiv a^2E/D$. (In the following we set $a=1$.)

This model will be investigated for one- and two-dimensional ($d=1$ and $d=2$) surfaces in the following. Note that it reduces to the usual model for molecular beam epitaxy growth (for a recent review see, e.g., Ref. [14]), if one does not distinguish the two particle types. Therefore, the D/F dependence of quantities like island density, adatom density, surface roughness, etc., are the same as usual. For general values of D/F and E/D we use kinetic Monte Carlo simulations [15,16] in order to investigate the model. However, for one-dimensional surfaces in the limit $D/F \to \infty$ we implemented a much more efficient algorithm, which is described in the Appendix.

III. CORRELATIONS OF THE *A* ATOMS

One of the most intriguing qualitative properties of this model is the time-periodic self-organization of A clusters on

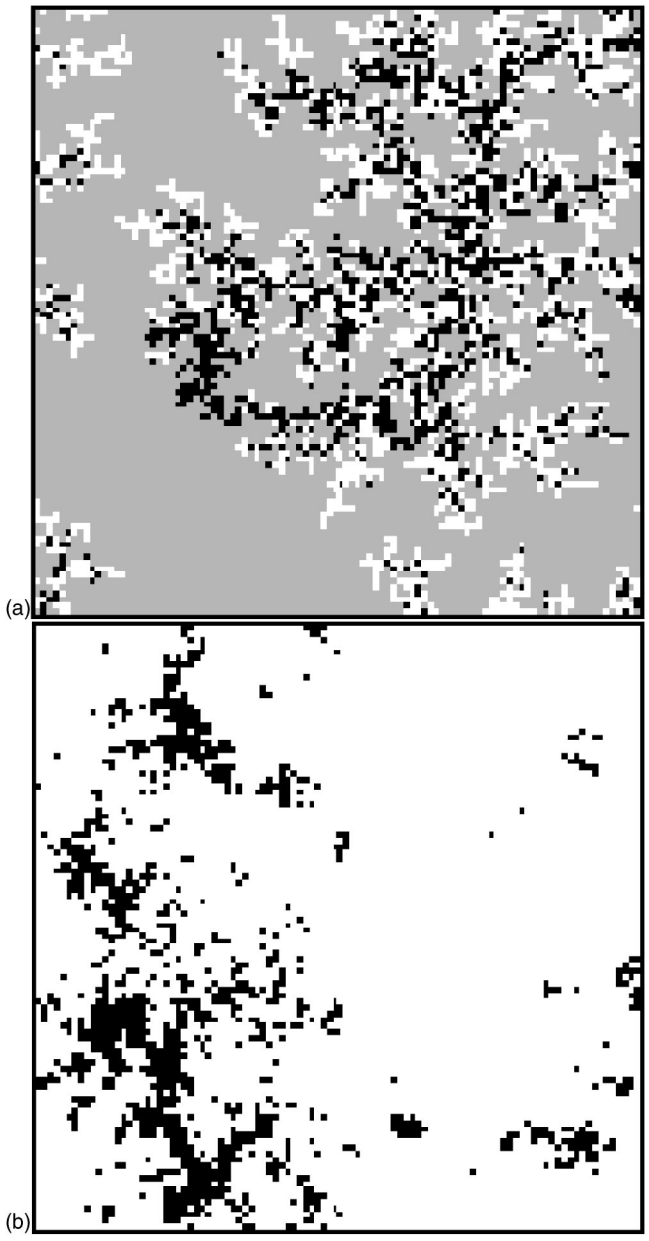

FIG. 2. Top view on the surface structure at $t=3.3$ ML (a) and $t=4.0$ ML (b). A atoms are black, B atoms are height encoded, where brighter means higher. $D/F=10^7$, $E/D=10^3$, $L^2=100\times100$.

the growing surface with a period of one monolayer. Figure 2 shows that the A atoms (black) are first clustered around the nucleation sites of a new layer, but migrate towards the holes remaining in that layer, when the islands coalesce. Thus, the characteristic distance between these clusters agrees with the typical distance between the nucleation sites, the diffusion length [17]:

$$\ell_D \sim (D/F)^{\gamma}, \tag{1}$$

as long as layer-by-layer growth persits. This can be verified by examining the lateral correlations of A atoms on the surface after deposition of t monolayers

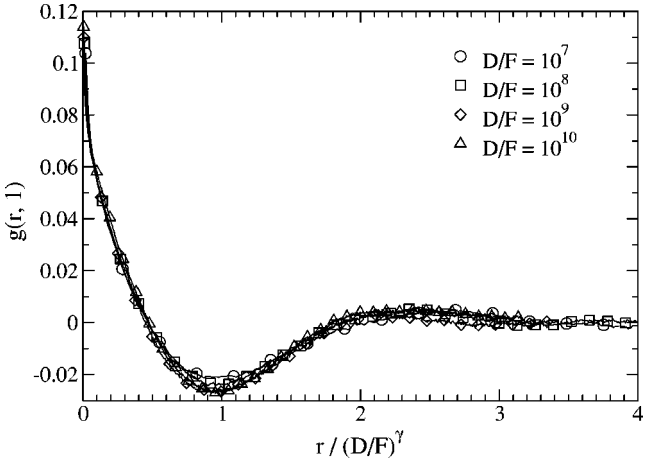

FIG. 3. Lateral A-A correlation functions $g(r,t)$ at $t=1$ for different D/F ($d=1$). The average distance between A clusters scales with D/F like the distance of the nucleation sites, Eq. (1), where $\gamma=1/4$ for $d=1$.

$$g(\boldsymbol{r},t)=\frac{1}{L^d}\sum_{x=1}^{L^d} n_A(\boldsymbol{x},t)n_A(\boldsymbol{x}+\boldsymbol{r},t)-c_A(t)^2, \tag{2}$$

where $n_A(\boldsymbol{x})=1$ if there is an A atom at surface site $\boldsymbol{x}$, and $n_A(\boldsymbol{x})=0$ if there is none. $c_A(t)$ denotes the surface density of A atoms. A data collapse of these correlation functions for different values of D/F is obtained, if the space coordinates are rescaled by ℓ_D (see Fig. 3 for $d=1$), which shows that this is the characteristic distance between the A clusters.

The mechanism of the periodic self organization can most clearly be seen in the limit $r_E=E/D\to\infty$, where every B adatom exchanges with the first exchange partner A it encounters. When layer t is completed and layer $t+1$ begins to grow, the first B atoms deposited are likely to exchange with A atoms from layer t. Hence, the nuclei of islands in the new layer $t+1$ will consist predominantly of A atoms. As growth proceeds, the lower terrace (layer t) gets depleted from exchange partners A, either because they are exchanged with freshly deposited B adatoms or get overgrown by the islands. Then the core of the islands with a high concentration of A atoms gets surrounded by mainly B atoms [Fig. 2(a)]. However, as the island size increases, it becomes more and more likely that B atoms are deposited on top of the islands, i.e., in layer $t+2$. These B adatoms find many exchange partners at the core of the islands, which then become "washed out" and start decorating the island edges, because there are no Ehrlich-Schwoebel barriers in our model. Note that this edge decoration with A atoms happens *without lateral exchange* of B with A atoms at the edges of the islands, in contrast to the situation studied in Ref. [18]. As a result, the interior of the islands gets cleared from A atoms, which are collected in the holes of layer $t+1$ which get filled last [Fig. 2(b)]. Then the process starts again: Layer $t+2$ nucleates predominantly with A atoms which were exchanged from layer $t+1$.

For finite r_E the mechanism is similar. However, for vicinal surfaces growing in step flow mode, the correlations among the A atoms are different. Here, the terraces get

cleared of A atoms, which attach to the step edges. This decoration of advancing edges leads to a correlation pattern $g(\boldsymbol{r},t)$ with a spatial periodicity identical to the width of the terraces.

The clustering of A atoms on the surface leads to correlations among the A atoms which get overgrown and hence incorporated as impurities into the B film. For vicinal surfaces growing in step flow mode these correlations are much weaker than for layer-by-layer growth on singular surfaces.

IV. THE SCALE FREE LIMIT

The limit of perfect layer-by-layer growth, $D/F\to\infty$, is particularly instructive. In this case, there is only one island on the surface, nucleating at a random site. Afterwards at most one adatom can be found on the surface at a time. If we assume maximal exchange in addition, i.e., an exchange rate E much larger than both D and F, $r_E=E/D\to\infty$, the model becomes parameter-free. A atoms can be buried even in this limit, when they are overgrown by an island edge. However, the last A atom will never get buried in this case. The nucleus of a new layer will always contain at least one of the remaining surface atoms of type A in the limit we focus on, because the first B atom deposited after completion of a layer exchanges with an A atom before the next B atom gets deposited: $c_A(t\to\infty)=L^{-d}$. As this case is scale free, we expect that the concentration of A atoms falls off like a power law into the growing B film.

In order to get a first idea about the distribution of A atoms in the growing B film, it suffices to consider the concentration $c_A(t)$ of A atoms at the surface after the deposition of *integer numbers* t of monolayers. During the growth of the next layer, a certain fraction $(1-q)\in[0,1)$ of these A atoms is transported to the next layer via vertical exchange

$$c_A(t+1)=(1-q)c_A(t). \tag{3}$$

If q was constant, this would imply an exponential decay $c_A(t)\propto(1-q)^t$. In the present model, however, the probability q that an A atom gets overgrown decreases with decreasing $c_A(t)$, resulting in a decay which is slower than exponential.

Qualitatively this can be understood in the following way: In the limit $D/F\to\infty$ there is only one island on the surface. Moreover, any A atom on the lower terrace gets transferred to the new layer as soon as it is reached by an adatom of type B, because $r_E\to\infty$ is assumed, as well. Only A atoms sufficiently close to the island have a chance to be overgrown by the island edge before being visited by a B atom.

The island edge advances a characteristic distance ℓ_{cover}, while the lower terrace gets depleted from A atoms by exchange with adatoms of type B. For a one-dimensional surface of length L it is clear that ℓ_{cover} is proportional to the number of A atoms at the surface, $c_A(t)L$. Hence, the number of A atoms with a chance to be overgrown is of the order of

$$\ell_{\text{cover}}c_A(t)\propto c_A(t)^2L. \tag{4}$$

This must be compared with $qc_A(t)L$, which shows that

$$q\propto c_A(t). \tag{5}$$

Inserting Eq. (5) into Eq. (3) leads to the difference equation

$$c_A(t+1)-c_A(t)\propto -c_A(t)^2 \tag{6}$$

implying the asymptotic power law

$$c_A(t)\sim 1/t \tag{7}$$

for the concentration of A atoms at the surface.

At time t the concentration of A atoms *not* transported further into layer $t+1$ is $c_A(t)-c_A(t+1)$. This is the concentration of A impurities incorporated into the B film at a distance $z=at/t_F$ from the substrate. As explained earlier we take a and t_F as units of length and time so that z can be identified with t. Hence, the concentration profile of impurity atoms inside the grown film is given by

$$-c_A'(t)=c_A(t)-c_A(t+1)\sim 1/t^2. \tag{8}$$

This implies that the average distance of impurity atoms from the substrate diverges logarithmically with the thickness $t_{\max}$ of the film

$$\langle z\rangle=-\sum_{t=1}^{t_{\max}-1}c_A'(t)t+c_A(t_{\max})t_{\max}\sim\ln t_{\max}. \tag{9}$$

Nevertheless, the interface can be localized precisely, because B atoms do not occur below layer $t=0$ due to the absence of bulk diffusion in this model. Later we show that these power laws are confirmed by simulations.

The argument leading to Eq. (5) ignores that the A atoms at the surface are clustered, as shown in Fig. 2, and was made plausible only for a one-dimensional surface. However, it can be refined such that it takes these spacial correlations into account and applies also for two-dimensional surfaces. For $D/F\to\infty$, we can imagine that there is only one cluster of size $c_A(t)L^d$ on the surface, when the new layer nucleates. The important point is that the nucleation happens anywhere on the surface with equal probability $1/L^d$ in this case. However, only if the nucleation site is within an area of about the size $2^dc_A(t)L^d$ centered at the middle of the cluster, there is a chance that some A atoms get overgrown. In other words, only a fraction of nucleation sites $\propto c_A(t)$ leads to overgrowth. The average number of A atoms overgrown in such a case is proportional to the cluster size. Hence, on average a fraction q of A atoms is overgrown which is proportional to the fraction of nucleation sites leading to overgrowth, i.e., this refined argument gives $q\propto c_A(t)$ as in Eq. (5).

V. THE WIDTH OF THE INTERDIFFUSION ZONE FOR $D/F\to\infty$

In the previous section we predicted that the mean distance of impurity atoms from the substrate diverges in the scale free limit, where $D/F\to\infty$ and $r_E\to\infty$. In this section we show that for finite r_E the power law Eq. (7) is only valid, if the system is infinitely large. For finite system size the power law is exponentially cut off at a characteristic distance H from the substrate. Above this height the remaining impurity atoms die out quickly by being incorporated into the

growing B film. Therefore, one can call H the *width of the interdiffusion zone*. It could be defined as the limit $n \to \infty$ of

$$\langle z^n \rangle^{1/n} = \left[-\sum_{t=1}^{\infty} c_A'(t) t^n \right]^{1/n} \sim H^{1-1/n}. \tag{10}$$

The average distance of impurity atoms from the substrate is given by $\langle z \rangle \sim \ln H$ instead of Eq. (9).

Now we derive the size and r_E dependence of H. After the completion of several monolayers on a substrate of linear size L the number of substrate atoms at the surface is $c_A L^d$. The A atoms are concentrated in a cluster, which we assume to be compact, hence, of diameter $\propto c_A^{1/d} L$. This assumption is justified even for $d=2$, where the islands initially are fractal, because the A cluster occupies the sites which were filled *last* in the uppermost monolayer. These sites do not form a fractal.

Now we imagine the surface to be coarse grained on the scale of the cluster diameter so that exactly one cell contains the A cluster. The typical residence time of an adatom in such a cell is

$$\Delta t = \frac{(c_A^{1/d} L)^2}{D}. \tag{11}$$

A B adatom which enters the cell containing the A cluster will almost certainly be replaced by an exchange partner A within the residence time, if

$$E \Delta t = r_E (c_A^{1/d} L)^2 \gg 1 \tag{12}$$

(exchange dominates). For $E\Delta t \ll 1$ the adatom changes from type B into type A only with probability $E\Delta t$ (overgrowth dominates).

It is plausible to assume that the power law belongs to the exchange dominated slow decay of c_A while the exponential cut off indicates the much faster decay when overgrowth dominates. Thus, the width H of the interdiffusion zone should be reached, when c_A becomes so small that exchange is no longer guaranteed, i.e., when $E\Delta t$ drops below 1. Inserting $c_A \approx 1/t = 1/H$ into Eq. (12) one obtains

$$H \approx (\sqrt{r_E} L)^d. \tag{13}$$

However, as c_A cannot become smaller than L^{-d}, this estimate is only valid for $r_E < 1$, while $H \approx L^d$ for $r_E > 1$. This is our prediction for the width of the interdiffusion zone in the limit $D/F \to \infty$. Note that in this limit the cut off of the power law is a finite size effect: For $L \to \infty$ the power law extends to infinity.

Based on the results of this and the previous paragraph we can conjecture the following scaling form for the surface concentration of A's:

$$c_A(t, L; r_E) - c_A(t \to \infty) = \frac{1}{H} f\left(\frac{t}{H}\right), \tag{14}$$

where according to Eq. (7):

$$f(\tau) \sim 1/\tau \quad \text{for} \quad \tau \ll 1. \tag{15}$$

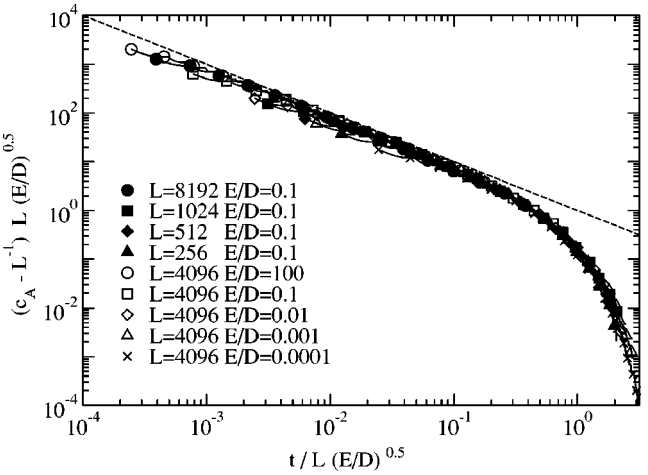

FIG. 4. Scaling of $c_A(t)$ with L and E/D in $d=1$ for $D/F \to \infty$. Full symbols mark four curves for $E/D=0.1$ and L between 256 and 8192. Open symbols mark five curves for $L=4096$ and E/D between 10^{-4} and 100. A data collapse of all nine curves is reached by scaling in accordance with Eqs. (14) and (13). The data for $E/D=100$ were rescaled differently: Here, $c_A L - 1$ is plotted vs t/L, as if E/D was 1 instead of 100. This shows, that H becomes independent of E/D for $E/D > 1$ as explained after Eq. (13). The dashed line has slope -1 in agreement with Eq. (15).

VI. NUMERICAL RESULTS FOR $D/F \to \infty$

In order to check the predictions of Secs. IV and V, we simulated the model described in Sec. II for $D/F \to \infty$ and varied the values of r_E and system size L for one- and two-dimensional surfaces. For the case $d=1$ we used the algorithm described in the Appendix, while kinetic Monte-Carlo simulations were done for $d=2$.

Figure 4 (for $d=1$) and Figs. 5 and 6 (for $d=2$) show the concentration c_A of A atoms at the surface as a function of deposition time t (in monolayers of B atoms). All curves are averages over 200–400 independent runs. Both for $d=1$ and $d=2$ the exponent of the power law decay was found to be

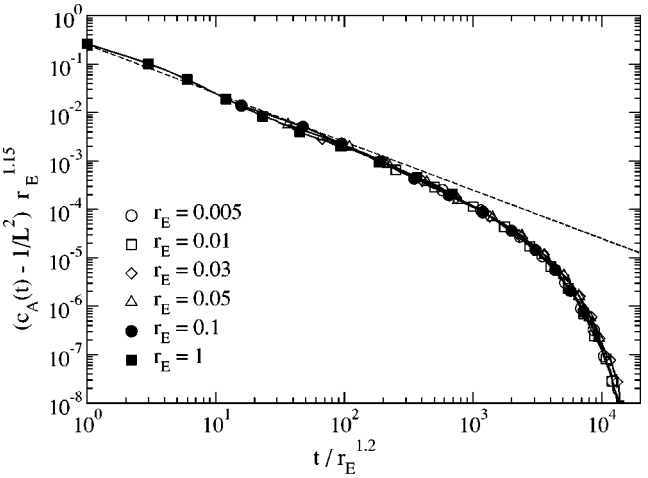

FIG. 5. Scaling of $c_A(t)$ with $r_E = E/D$ in $d=2$ for $D/F \to \infty$. $L^2 = 200 \times 200$. Dashed line has slope -1 in agreement with Eq. (15).

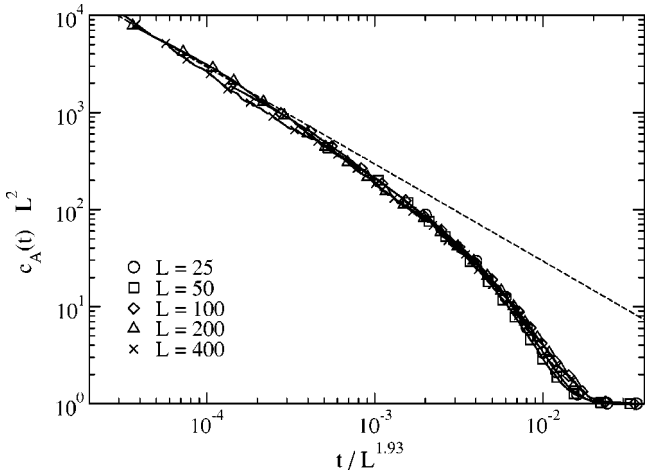

FIG. 6. Scaling of $c_A(t)$ with L in $d=2$ for $D/F \to \infty$. $E/D=0.1$. Dashed line has slope -1 in agreement with Eq. (15).

consistent with the value -1 derived in Sec. IV.

As shown in Fig. 4, the predicted relations Eqs. (13) and (14) lead to the expected data collapse for the one dimensional surface. The results in two dimensions are not as clear. In this case, we obtain the best data collapse with

$$H \propto L^{1.93}\, r_E^{1.2}, \tag{16}$$

as shown in the Figs. 5 and 6, whereas our predicted exponents [2 and 1, respectively, see Eq. (13)] were about 4% and 20% different. In fact, the A clusters are not as compact as assumed in the simple argument of Sec. V (see Fig. 2).

VII. SCALING FOR FINITE D/F

For finite D/F there are many A clusters on the surface. Their typical distance is given by the diffusion length ℓ_D as shown in Sec. III. The average size of the A clusters is $c_A \ell_D^d$, provided this is much larger than 1. If the concentration c_A becomes too small, less and less A clusters will be found on the surface, and their typical distance will grow. Finally all A atoms will be overgrown, in contrast to the situation of perfect layer-by-layer growth, where the last A atom could never be overgrown. Apart from this, one might expect that the results of the previous three sections would essentially remain true, if one replaces L by ℓ_D. Qualitatively, the surface concentration c_A indeed decays first approximately as a power law of the deposition time, with a cutoff at a characteristic width H of the interdiffusion zone.

Quantitatively, however, the situation turns out to be more complex than this: All exponents are different. The power law decay

$$c_A \propto t^{-\beta} \tag{17}$$

extends over at most two decades for the largest values of D/F we simulated, so that the determination of the exponent β from the slopes in the log-log plots of Fig. 7 ($d=1$) and Fig. 8 ($d=2$) is not very accurate. We estimate

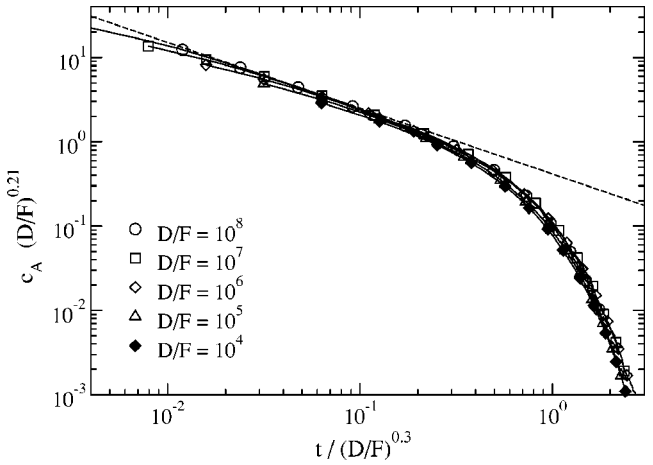

FIG. 7. Scaling of $c_A(t)$ with D/F in $d=1$. $E/D=10^3$, $L=5\times10^3 \ldots 10^4$. The dashed line indicates the exponent $\beta=0.78$.

$$\beta = \begin{cases} 0.78 \pm 0.08 & \text{for} \quad d=1, \\ 0.53 \pm 0.05 & \text{for} \quad d=2, \end{cases} \tag{18}$$

which are indicated by the dashed lines in the two figures. Both exponents are significantly smaller than $\beta=1$ obtained for infinite D/F, i.e., c_A decays more slowly for finite than for infinite D/F.

This result is surprising on first sight, because there are more island edges on the surface for finite D/F, hence, more possible places, where A atoms may be overgrown. That c_A decays more slowly nevertheless, may be explained by the fact, that the nucleation of islands does not happen anywhere with equal probability as for infinite D/F but preferentially far away from the holes in the previous layer, where the A atoms are concentrated. Therefore, overgrowth is less likely, and c_A decays more slowly than for infinite D/F.

This raises the question, how big the parameter D/F must be in order to see the exponent $\beta=1$ instead of the smaller one. The answer is, that the system size L must be small compared to ℓ_D in order to obtain the crossover to the faster decay of c_A. This was confirmed by simulation results in Ref.

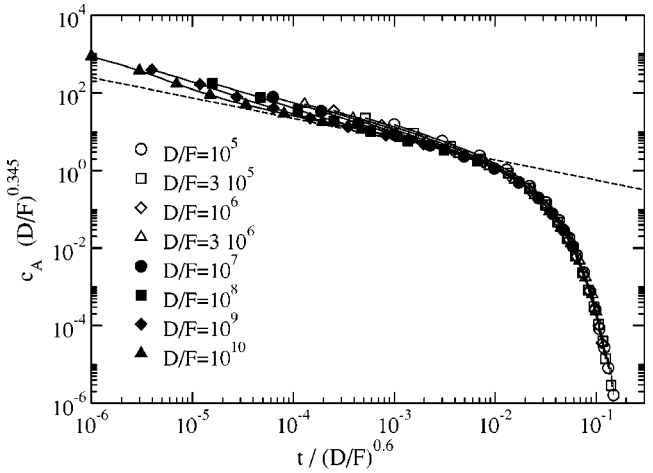

FIG. 8. Scaling of $c_A(t)$ with D/F in $d=2$. $E/D=10^4$, $L^2=500\times500$. The dashed line indicates the exponent $\beta=0.53$.

[19]. In the four figures belonging to this section we carefully checked that the system sizes were big enough to exclude finite size effects.

Because the impurity concentration falls off more slowly for finite D/F, Eq. (10) is replaced by

$$\langle z^n\rangle^{1/n} = \left[-\sum_{t=1}^{\infty} c_A'(t) t^n \right]^{1/n} \sim H^{1-\beta/n}. \tag{19}$$

The limit $n \to \infty$ can still be used as a definition of the width H of the interdiffusion zone. The average distance of the impurities from the substrate is now

$$\langle z\rangle \sim H^{1-\beta}. \tag{20}$$

In analogy to Eq. (12) we expect that the power law decay of $c_A \propto t^{-\beta}$ stops, when

$$r_E (c_A \ell_D^d)^{2/d} \approx 1, \tag{21}$$

or

$$c_A \ell_D^d \approx 1, \tag{22}$$

whichever happens first. Replacing c_A by $H^{-\beta}$, this implies that the width H of the interdiffusion zone should be given by

$$H \approx \ell_D^{d/\beta} \quad \text{for} \quad r_E \gg 1 \tag{23}$$

and

$$H \approx (\sqrt{r_E}\ell_D)^{d/\beta} \quad \text{for} \quad r_E \ll 1. \tag{24}$$

In analogy to Eq. (14) we postulate then that

$$c_A = \frac{1}{H^\beta} g\left(\frac{t}{H}\right) \tag{25}$$

with

$$g(\tau) \sim 1/\tau^\beta \quad \text{for} \quad \tau \ll 1, \tag{26}$$

because c_A is independent of H for small t.

We first checked these conjectures for $r_E > 1$, where the surface concentration of A's becomes independent of r_E, as expected. If we insert the D/F-dependence Eq. (1) of the diffusion length in Eq. (23), Eq. (25) can be written in the form

$$c_A \left(\frac{D}{F}\right)^{\gamma d} = g_1\left(t\left(\frac{D}{F}\right)^{-\gamma d/\beta}\right). \tag{27}$$

With $\gamma = 1/4$ [20] for $d=1$ and $\gamma = 1/(4+d_f) \approx 0.17$ for $d=2$ (d_f is the fractal dimension of the islands) [21], and with the β values determined earlier, the theory predicts

$$\gamma d = \begin{cases} 0.25 & \text{for} \quad d=1 \\ 0.35 \pm 0.01 & \text{for} \quad d=2, \end{cases} \tag{28}$$

$$\gamma d/\beta = \begin{cases} 0.32 \pm 0.03 & \text{for} \quad d=1 \\ 0.66 \pm 0.07 & \text{for} \quad d=2. \end{cases} \tag{29}$$

The data collapses in Figs. 7 and 8 are in reasonable agreement with this prediction.

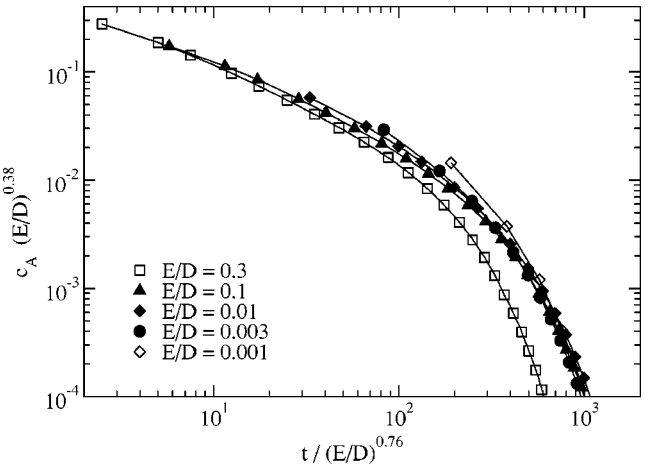

FIG. 9. Scaling of $c_A(t)$ with E/D in $d=1$. $D/F=10^7$, $L=5\times10^3$.

However, the r_E-dependence Eq. (24) for $r_E<1$ is not in agreement with the simulation results. For fixed D/F the theory Eq. (25) predicts

$$c_A r_E^{d/2} = g_2(t\, r_E^{-d/2\beta}). \tag{30}$$

Inserting the value of β determined earlier, the scaling exponent should be

$$d/2\beta = \begin{cases} 0.64 \pm 0.06 & \text{for} \quad d=1 \\ 1.9 \pm 0.2 & \text{for} \quad d=2. \end{cases} \tag{31}$$

For $D/F=10^7$ we could only check this for about one decade of r_E values: For $d=1$ we found that already for $r_E=0.3$ the crossover into the regime, where H becomes independent of r_E, affects the data. For $r_E<10^{-3}$ the exchange was so weak that the surface concentration of A's decayed very fast from the beginning, so that a convincing data collapse was not possible. Similar problems occurred for $d=2$. The best result of our attempts to get a data collapse in the available r_E interval are shown in Fig. 9 for $d=1$ and Fig. 10 for $d=2$.

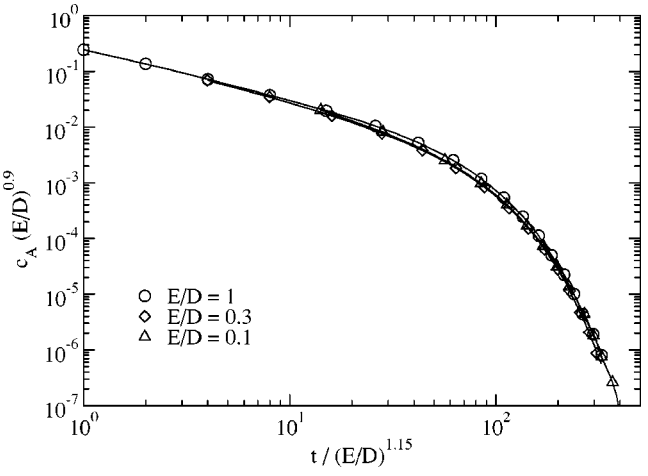

FIG. 10. Scaling of $c_A(t)$ with E/D in $d=2$. $D/F=10^7$, $L^2=500\times500$.

The effective exponents turn out to be very different from the ones predicted in Eq. (30).

VIII. RATE EQUATION APPROACH

In this section we extend the established rate equation approach for submonolayer homoepitaxial growth as described in Refs. [22] and [23], in order to apply it to our model for surface interdiffusion. Our approach describes the time evolution of four submonolayer quantities: The density of mobile adatoms ρ, the total island density I, the density of mobile adatoms of type B, ρ_B, and the density of potential exchange partners of type A in the lower layer, ρ_A. With these quantities, the rate equations are as follows:

$$\dot{\rho} = F - D\rho(I + 2\rho), \tag{32}$$

$$\dot{I} = D\rho^2, \tag{33}$$

$$\dot{\rho}_B = F - D\rho_B(I + \rho + \rho_B) - Ea^2\rho_A\rho_B, \tag{34}$$

$$\dot{\rho}_A = -Ea^2\rho_A\rho_B - \rho_A a^2 D\rho(I + 2\rho). \tag{35}$$

While the first two equations are identical to the well known point-island model rate equations for homoepitaxial growth, the last two are specific to our heteroepitaxial model. The third one expresses the change in density of the B-type adatoms. Its positive contribution describes the deposition of new adatoms. The first negative term represents the loss of B adatoms, when they get incorporated into islands or bind to another adatom to nucleate a new island. The extra term $D\rho_B^2$ accounts for the fact that nucleation events involving two B adatoms count twice as much as those between a B and an A adatom, because they remove two B adatoms simultaneously. The last term of Eq. (34) describes the exchange of mobile B's with A's. Equation (35) expresses the annihilation of possible A-type exchange partners in the lower layer. Since this value is monotonously decreasing, there is no positive contribution. The negative terms describe the exchange of A's with mobile B's, and the overgrowth of A's due to propagating island edges and nucleation events.

Rescaling the variables (see Ref. [22]) according to $\hat{t} = tF\ell_0^2$, $\hat{\rho} = \rho\ell_0^2$, $\hat{I} = I\ell_0^2$, $\hat{\rho}_A = \rho_A\ell_0^2$, $\hat{\rho}_B = \rho_B\ell_0^2$, where $\ell_0 = (D/F)^{1/4}$, leads to the dimensionless equations

$$\dot{\hat{\rho}} = 1 - \hat{\rho}(\hat{I} + 2\hat{\rho}), \tag{36}$$

$$\dot{\hat{I}} = \hat{\rho}^2, \tag{37}$$

$$\dot{\hat{\rho}}_B = 1 - \hat{\rho}_B(\hat{I} + \hat{\rho} + \hat{\rho}_B) - r_E\hat{\rho}_A\hat{\rho}_B, \tag{38}$$

$$\dot{\hat{\rho}}_A = -r_E\hat{\rho}_A\hat{\rho}_B - (a/l_0)^2\hat{\rho}_A\hat{\rho}(\hat{I} + 2\hat{\rho}). \tag{39}$$

If we consider systems in perfect layer-by-layer growth mode, this approach not only holds for the submonolayer regime starting from the substrate, but also starting after integer numbers of deposited monolayers. The initial conditions of these equations for a flat surface after n deposited monolayers are

$$\hat{\rho}(0) = \hat{I}(0) = \hat{\rho}_B(0) = 0, \quad \hat{\rho}_A(0) = \hat{c}_A(n). \tag{40}$$

Disregarding the point island model nature of this approach, which only holds for early stages of the submonolayer regime, we can establish the surface concentration of A's after the deposition of one additional monolayer, $c_A(n+1)$, as the integral over the density of all exchanged atoms

$$\hat{c}_A(n+1) = \int_0^{(\ell_0/a)^2} d\hat{t}\, r_E\hat{\rho}_A\hat{\rho}_B. \tag{41}$$

The upper integration boundary is the dimensionless time for depositing one monolayer. This approximation can be justified by taking into account that the transport of A atoms from the nth to the $(n+1)$th layer mainly takes place at early times, that is, the nucleation regime and early stages of the intermediate coverage regime, as explained in Sec. III. The chosen approach describes these regimes with sufficient accuracy.

The solution of the first two equations can be taken directly from the literature [23]: For early times, $\hat{t} \ll 1$, $\hat{\rho}$ is linear in $\hat{t}$, and $\hat{I}$ increases with $\hat{t}^3$. At late times, $\hat{t} \gg 1$, one gets $\hat{\rho} \propto \hat{t}^{-1/3}$ and $\hat{I} \propto \hat{t}^{1/3}$.

With these results, the last two equations can be solved analytically in a similar way for the early-time regime, $\hat{t} \ll 1$. For Eq. (38), the second term on the right hand side can be neglected in this limit. If we also neglect the time dependence of $\hat{\rho}_A(t) \approx \hat{\rho}_A(0) = \hat{c}_A(n)$, we get

$$\dot{\hat{\rho}}_B \approx 1 - r_E\hat{c}_A\hat{\rho}_B. \tag{42}$$

This equation relaxes into a steady state with $\hat{\rho}_{B,\infty} \propto 1/(r_E\hat{c}_A)$ after a characteristic time $\hat{t}^* \approx 1/[r_E\hat{c}_A(n)]$. For even smaller times, $\hat{t} \ll \hat{t}^*$, we can also neglect the other right hand side term, and we get $\hat{\rho}_B \propto \hat{t}$.

Plugging these results into Eq. (39), and realizing that the second term on the right hand side can be neglected compared to the first one, we get

$$\hat{\rho}_A \propto e^{-\hat{t}/\hat{c}_A} \approx \left(1 - \frac{\hat{t}}{\hat{c}_A}\right) \text{ for } \hat{t}^* \ll \hat{t} \ll 1 \tag{43}$$

and

$$\hat{\rho}_A \propto e^{-r_E\hat{t}^2} \approx (1 - r_E\hat{t}^2) \text{ for } \hat{t} \ll \hat{t}^*. \tag{44}$$

To relate these findings to our results in the other sections, we employed an iteration scheme for the rate equation system to obtain the surface concentration of A's for every deposited integer monolayer. Starting from the substrate $[\rho_A(0) = c_A(0) = 1]$ we can obtain $\rho_A(1) = c_A(1)$ from Eq. (41) by solving Eqs. (36)–(39) numerically. Plugging $c_A(1)$ back into our rate equations as the initial surface concentration, that is $\rho_A(0) = c_A(1)$, we get $\rho_A(1) = c_A(2)$ by using Eq. (41) again. Repeating this iteration scheme leads to $c_A(t)$.

The rescaled results of this approach for different D/F are shown in Fig. 11. One can clearly observe power law decay for high D/F values at intermediate times, and a similar

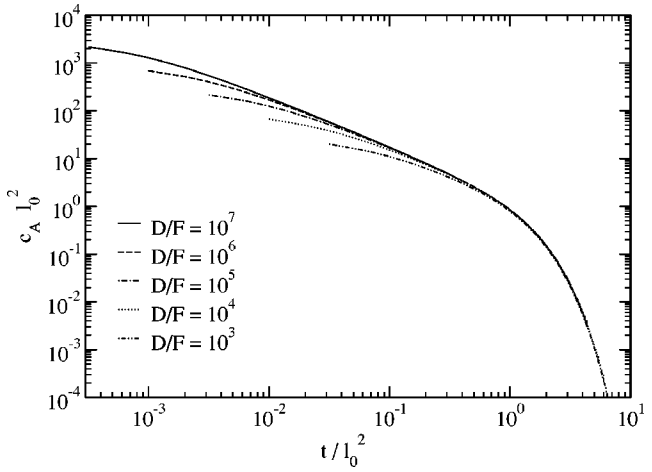

FIG. 11. Scaled time dependence of the surface concentration of substrate atoms, obtained from the iteration of the rate equations. The slope of the power law region is -1.03 ± 0.05. $E/D=1$.

scaling behavior as obtained from the simulations. The exponent of the power law behavior is approximately -1, which is identical to the result from the simulations for perfect layer-by-layer growth mode, $D/F\to\infty$. This fact supports our argumentation concerning the different exponents for $D/F\to\infty$ and finite D/F in Sec. VII: Since the rate equations cannot describe the clustering of the A atoms, they also do not reflect the preference of the nucleation sites to be far from the A clusters. The observed scaling exponent of $l_0^2=(D/F)^{1/2}$ does not match any of the exponents resulting from the simulations. This is in general agreement with the analytical calculation of the exponents in Sec. V: There we derived the scaling exponents from characteristic properties of the A clusters, which are totally neglected in the presented rate equation approach.

IX. CONCLUSION

In the present work we have investigated heteroepitaxial growth of B particles on an A substrate. Introducing an exchange mechanism for B adatoms, when they encounter an A atom in the uppermost layer, we observed that in the limit of layer-by-layer growth the top layer concentration of A atoms decays algebraically like $t^{-\beta}$. We obtained the exponent $\beta\approx0.8$ for $d=1$ and $\beta\approx0.5$ for $d=2$, independent of the rate E at which A atoms and B atoms are exchanged. This is smaller than the mean field exponent $\beta=1$ obtained from rate equation analysis and in the limit $D/F\to\infty$ for fixed system size.

For finite values of D/F a crossover from power law to exponential decay was found. The crossover time H (which we identified with the width of the interdiffusion zone) is approximately proportional to $(D/F)^{0.3}$ for $d=1$ and to $(D/F)^{0.6}$ for $d=2$ and also increases with E/D.

An intriguing consequence of our findings is that we predict the possibility of a nonmonotonous temperature dependence of H: Whereas one expects that the interdiffusion zone becomes wider with increasing temperature, it may actually become narrower in certain cases. With the effective exponents obtained for a two dimensional surface in Figs. 8 and 10 the width of the interdiffusion zone should be approximately proportional to

$$H\propto\left(\frac{E}{D}\right)^{1.2}\left(\frac{D}{F}\right)^{0.6}, \tag{45}$$

provided $E/D<1$. The exchange and diffusion rates should follow Arrhenius laws with activation energies E_E and E_D, respectively, and attempt frequencies ν_E and ν_D assumed to be independent of temperature, i.e.:

$$E=\nu_E\exp\left(-\frac{E_E}{k_BT}\right),\quad D=\nu_D\exp\left(-\frac{E_D}{k_BT}\right) \tag{46}$$

so that

$$H\propto\left(\frac{\nu_E^2}{\nu_D F}\exp\left[-\frac{2E_E-E_D}{k_BT}\right]\right)^{0.6}. \tag{47}$$

The interesting case is that the activation energy for the exchange of a B adatom with an A atom underneath is smaller than the activation energy for surface diffusion, $2E_E<E_D$, and at the same time the attempt frequency for exchange is smaller than the one for diffusion, too. Then there is a reversal temperature T_{rev} up to which the width of the interdiffusion zone increases, and above which it becomes smaller again. T_{rev} is given by

$$k_BT_{\mathrm{rev}}\approx\frac{E_D-E_E}{\ln\,\nu_D-\ln\,\nu_E}. \tag{48}$$

For $T<T_{\mathrm{rev}}$ the condition $E/D<1$ is violated, so that H does not depend on E/D and therefore increases with increasing temperature. For $T>T_{\mathrm{rev}}$, however, Eq. (45) applies. According to Eq. (47) this means that H decreases again.

How robust are these results, if the simplifying assumptions made in this investigation are relaxed? Let us first discuss the case that impurity atoms diffuse faster than B atoms on the surface of the B film, $D_A>D_B$. As long as A-exchange partners are available for B adatoms, one should get nucleation of islands consisting predominantly of A atoms as explained in Sec. III. After sufficient depletion of exchange partners one will get secondary nucleation of essentially pure B islands on a smaller length scale. This should enhance the probability for overgrowth so that we expect a larger exponent β in this case, perhaps as large as the mean field value, $\beta=1$.

If $D_A<D_B$, no such nucleation of secondary islands is expected. The islands nucleating at the beginning of a new monolayer have a distance corresponding to the diffusion length of the A adatoms. At the later stage of monolayer filling, when B adatoms no longer find exchange partners, they attach to the already existing islands so that their diffusion length gets effectively reduced to the distance between the islands. Therefore, we expect that the case $D_A<D_B$ is very similar to the case $D_A=D_B$ studied in this paper.

If Ehrlich-Schwoebel barriers inhibit interlayer diffusion, a flat surface will be unstable with respect to three-dimensional mound formation. This instability predicted by Villain [24] has been observed in many systems [25]. However, the weaker the Ehrlich-Schwoebel barrier is, the later the instability sets in. One observes damped layer-by-layer

growth oscillations up to a characteristic film thickness $\tilde{t}$ which is an increasing function of $D/(F\ell_s^{2.8})$ [26], where ℓ_s is the so-called Schwoebel length and is a measure for the strength of the Ehrlich-Schwoebel barriers. If $\tilde{t}$ is larger than the width H of the interdiffusion zone calculated in this paper without Ehrlich-Schwoebel barriers, the Villain instability sets in too late to change the results we obtained. This was shown by recent simulations of the interdiffusion model which included Ehrlich-Schwoebel barriers [27].

These arguments show, that the impurity profile due to the partial surfactant behavior investigated in this paper should be observable in real systems in spite of the simplifying assumptions we made.

ACKNOWLEDGMENTS

The authors are very grateful to H. Hinrichsen, L. Brendel, V. Uzdin, U. Koehler, C. Wolf, and A. Lorke, with whom they had many fruitful discussions. This work was supported by the DFG within Sonderforschungsbereich 491 (Magnetic Heterolayers) and GK 277 (Strukture and Dynamics of Heterogeneous Systems), as well as by the INTAS-Project No. 2001-0386. Work done by S.B.L. was supported in part by Korea Research Foundation Grant No. (KRF-2001-015-DP0120).

APPENDIX

Here we describe, how we implemented the model introduced in Sec. II for one-dimensional surfaces in the limit $D/F\to\infty$. We first describe the idea for the scale free limit, where also $E/D\to\infty$.

For $D/F\to\infty$ one has perfect layer-by-layer growth. The nucleation of a new layer happens at an arbitrary position. Afterwards there is at most one adatom on the surface. The idea is to calculate the probabilities exactly, with which the adatom reaches the nearest sinks to its left and to its right. For an A adatom these are the island edges, while for a B adatom it might also be an A atom, with which it could exchange. Let d_L (d_R) denote the distance to the nearest sink to the left (right).

As shown in Ref. [28], the probability p_L to reach the left position prior to the right one with unbiased diffusion is given by

$$p_L = \frac{d_R}{d_R + d_L}. \tag{A1}$$

Correspondingly, $p_R = 1 - p_L$. Therefore, it is not necessary to simulate the whole random walk of an adatom, but it suffices to select the final position according to Eq. (A1).

Thus, in the scale free limit the model (after nucleation of a new layer) may be simulated as follows:

(1) Deposition of a B at a randomly chosen site i.

(2) Determination of the distances d_L and d_R followed by a decision for a side according to the probabilities given in Eq. (A1).

(3) If the final position of the B adatom is an A site, the atoms exchange (as $E/D\to\infty$). In this case the A adatom goes to the left or right island edge according to Eq. (A1). If the final position of the B adatom is an island edge, it is bound there irreversibly possibly overgrowing an A atom. Then one returns to step (1) and deposits the next B atom.

This algorithm can be generalized for finite $r_E = E/D$: Not always, when a B adatom encounters an exchange partner A, they exchange immediately. This happens only with probability $p_E = E/(E+2D)$, where the denominator is the sum of the rates for the three possible actions of the adatom—exchange with the A atom underneath, a hop to the right neighbor and a hop to the left neighbor. With probability p_E the B adatom is replaced by an A adatom, which attaches to the island edges to its left with probability Eq. (A1), and otherwise to the island edge to its right; $1-p_E$ is the probability that the B adatom continues to diffuse until it encounters the next A atom or attaches to the island edge.

In order to avoid simulating the random walk explicitly, one has to calculate the probabilities analytically, that the B adatom exchanges with any particular of the A atoms or attaches to the island edges. Technically speaking, the B atom is a random walker on a one-dimensional lattice with fixed partial absorbers (the A atoms) and two full absorbers (the island edges) (Rosenstock trapping model with partial absorbers). In order to calculate the absorption probabilities at the different absorbers, which depend on the deposition site, we consider an incoming flux (normalized to 1) of independent random walkers at the deposition site x_S (source) and determine the outgoing fluxes at the absorption sites (sinks). The absorption probability is then the steady state fraction of the incoming flux that leaves the system at the respective absorption site.

The density of random walkers at a site x evolves according to

$$\dot{\rho}(x,t) = D[\rho(x-1,t) - 2\rho(x,t) + \rho(x+1,t)] - E\rho(x,t)\rho_A(x) + \delta_{x,x_S}, \tag{A2}$$

where the density of partial absorbers, $\rho_A(x)$, is 1 at the n sites $x_{A\nu}$, where an A atom sits, and 0 otherwise

$$\rho_A(x) = \sum_{\nu=1}^{n} \delta_{x,x_{A\nu}}. \tag{A3}$$

The terms on the right of Eq. (A2) which are proportional to D are the gain and loss terms due to hopping from a neighbor site to x, respectively, away from x. The term proportional to the exchange rate E describes the loss of walkers at the partial absorption sites. The last term is the gain term due to the normalized influx of walkers at site x_S. The perfect sinks corresponding to the island edges are represented by the boundary conditions $\rho(1) = \rho(L) = 0$, where L is the size of the terrace, on which the source is located.

The probability of absorption at site x_A is then obtained from the steady state solution of Eq. (A2) by

$$p(x_A) = E\rho(x_A), \tag{A4}$$

and the ones at the island edges by

$$p(1) = D\rho(2), \quad p(L) = D\rho(L-1). \tag{A5}$$

Introducing the diffusion current between x and $x+1$ (i.e., the current to the right of x and to the left of $x+1$):

$$j_R(x) = j_L(x+1) = -D[\rho(x+1) - \rho(x)], \tag{A6}$$

Eq. (A2) can be rewritten in the steady state as

$$j_R(x) - j_L(x) = -E\rho(x)\sum_{\nu=1}^{n} \delta_{x,x_{A\nu}} + \delta_{x,x_S}. \tag{A7}$$

This shows that $\rho(x)$ is a piecewise linear function with slope discontinuities at the source and the sinks. Hence, Eq. (A2) reduces to a set of $2n+2$ coupled linear equations for the $2n+2$ unknowns $j_R(x_{A\nu}), \rho(x_{A\nu})$ and the boundary values $j_R(1)$ and $j_L(L)$.

The solution determines the probabilities Eqs. (A4) and (A5) with which a freshly deposited B atom is exchanged at the different A sites or absorbed by the island edges. By choosing a random number we decide which site to pick. If it is an island edge, the B atom is moved there, and the next B atom is deposited at a random position. Otherwise, we move the B atom to the chosen site, exchange it with the A atom there, let another random number determine, whether to attach the A atom to the left or right island boundary, and deposit the next B atom at a random position.

The complexity of this algorithm is linear in the number of A atoms left on the surface, while a brute force simulation of the diffusion would cost much more computing time proportional to L^2.

[1] U. Nowak, A. Misra, and K. D. Usadel, J. Magn. Magn. Mater. **240**, 243 (2002).
[2] F. S. Bergeret, K. B. Efetov, and A. I. Larkin, Phys. Rev. B **62**, 11872 (2000).
[3] M. N. Baibich, J. M. Broto, A. Fert, F. NguyenVanDau, F. Petroff, P. Etienne, G. Creuzet, A. Friederich, and J. Chazelas, Phys. Rev. Lett. **61**, 2472 (1988).
[4] G. Binasch, P. Grünberg, F. Saurenbach, and W. Zinn, Phys. Rev. B **39**, 4828 (1989).
[5] F. S. Bergeret, A. F. Volkov, and K. B. Efetov, Phys. Rev. Lett. **86**, 3140 (2001).
[6] S. A. Wolf, D. D. Awschalom, R. A. Buhrmann, J. M. Daughton, S. von Molnar, M. L. Roukes, A. Y. Chtchelkanova, and D. M. Treger, Science **294**, 1488 (2001).
[7] V. M. Uzdin and C. Demangeat, Phys. Rev. B **66**, 092408 (2002).
[8] D. Venus and B. Heinrich, Phys. Rev. B **53**, R1733 (1996).
[9] M. Krishnamurthy, A. Lorke, and P. M. Petroff, Surf. Sci. Lett. **304**, L493 (1994).
[10] C. Wolf and U. Köhler, Surf. Sci. **523**, L59 (2003).
[11] M. M. J. Bischoff, T. Yamada, A. J. Quinn, R. G. P. van der Kraan, and H. van Kempen, Phys. Rev. Lett. **87**, 246102 (2001).
[12] K. Schroeder, A. Antons, R. Berger, and S. Blugel, Phys. Rev. Lett. **88**, 046101 (2002).
[13] G. L. Kellog, Surf. Sci. Rep. **21**, 1 (1994).
[14] A. C. Levi and M. Kotrla, J. Phys.: Condens. Matter **9**, 299 (1997).
[15] *Monte Carlo Methods in Statistical Physics*, edited by K. Binder (Springer, Heidelberg, 1986).
[16] M. E. J. Newman and G. T. Barkema, *Monte Carlo Methods in Statistical Physics* (Oxford University Press, New York, 1999).
[17] J. A. Venables, G. D. Spiller, and M. Hanbücken, Rep. Prog. Phys. **47**, 399 (1984).
[18] M. Kotrla, J. Krug, and P. Smilauer, Phys. Rev. B **62**, 2889 (2000).
[19] B. Bierwald, diploma thesis, Gerhard-Mercator-University Duisburg, 2002.
[20] A. Pimpinelli, J. Villain, and D. E. Wolf, Phys. Rev. Lett. **69**, 985 (1992).
[21] J. Villain, A. Pimpinelli, and D. E. Wolf, Comments Condens. Matter Phys. **16**, 1 (1992).
[22] L. H. Tang, J. Phys. I **3**, 935 (1993).
[23] J. G. Amar, F. Family, and P.-M. Lam, Phys. Rev. B **50**, 8781 (1994).
[24] J. Villain, J. Phys. I **1**, 19 (1991).
[25] T. Michely and J. Krug, *Islands, Mounds and Atoms* (Springer, Berlin, 2003).
[26] L. Brendel, A. Schindler, M. von den Driesch, and D. E. Wolf, Comput. Phys. Commun. **147**, 111 (2002).
[27] R. Zinetullin, diploma thesis, University of Duisburg-Essen 2003.
[28] C. W. Gardiner, *Handbook of Stochastic Methods* (Springer, Heidelberg, 1985).